^{31}P-Magnetization Transfer Magnetic Resonance Spectroscopy Measurements of In Vivo Metabolism

Douglas E. Befroy,[1,2] Douglas L. Rothman,[1,3] Kitt Falk Petersen,[2] and Gerald I. Shulman[2,4,5]

Magnetic resonance spectroscopy offers a broad range of noninvasive analytical methods for investigating metabolism in vivo. Of these, the magnetization-transfer (MT) techniques permit the estimation of the unidirectional fluxes associated with metabolic exchange reactions. Phosphorus (^{31}P) MT measurements can be used to examine the bioenergetic reactions of the creatine-kinase system and the ATP synthesis/hydrolysis cycle. Observations from our group and others suggest that the inorganic phosphate (P_i) → ATP flux in skeletal muscle may be modulated by certain conditions, including aging, insulin resistance, and diabetes, and may reflect inherent alterations in mitochondrial metabolism. However, such effects on the P_i → ATP flux are not universally observed under conditions in which mitochondrial function, assessed by other techniques, is impaired, and recent articles have raised concerns about the absolute magnitude of the measured reaction rates. As the application of ^{31}P-MT techniques becomes more widespread, this article reviews the methodology and outlines our experience with its implementation in a variety of models in vivo. Also discussed are potential limitations of the technique, complementary methods for assessing oxidative metabolism, and whether the P_i → ATP flux is a viable biomarker of metabolic function in vivo. ***Diabetes*** **61:2669–2678, 2012**

Because of its versatility, magnetic resonance spectroscopy (MRS) has emerged as a powerful modality for studying tissue-specific intracellular metabolism in vivo. Several metabolically relevant nuclei, including hydrogen (^{1}H), carbon (^{13}C), and phosphorus (^{31}P), are magnetic resonance (MR)-visible, permitting the detection of a range of metabolites in a variety of tissues. The noninvasive nature of the technique allows repeated measurements from the same location, so that the response to an acute intervention (e.g., exercise, insulin stimulation) or longer-term treatment (e.g., diet manipulation, drug therapy) can be assessed. Using more sophisticated MRS techniques, discrete reaction rates can also be estimated using ^{13}C-MRS to monitor the metabolic fate of ^{13}C-labeled substrates or by using magnetization-transfer (MT) techniques to monitor the unidirectional fluxes associated with metabolic exchange reactions. Of these, ^{31}P-MT methods offer the ability to examine the key bioenergetic reactions of the creatine kinase (CK) equilibrium (ATP ⇆ phosphocreatine [PCr] exchange) and the ATP synthesis/hydrolysis cycle (ATP ⇆ inorganic phosphate [P_i] exchange). Particular interest has been generated by the observations from our group and others that unidirectional P_i → ATP flux in muscle may be modulated in certain disease states, including insulin resistance and diabetes, that may reflect alterations in mitochondrial metabolism. However, disparate results have been reported by different groups, and recent articles have raised concerns about the absolute magnitude of the measured reaction rates. Given that many clinical MR scanners now have the capability of performing ^{31}P-MT experiments and the implementation of the method is becoming more widespread, we would like to offer our perspective on the application of the technique in vivo. In this article, we review our experience using the ^{31}P-MT technique to measure P_i → ATP flux in a variety of models, describe limitations of the methodology, assess alternative and complementary methods of estimating cellular bioenergetics, and discuss the validity of using the technique as a biomarker of metabolic function in vivo.

From the [1]Department of Diagnostic Radiology, Yale University School of Medicine, New Haven, Connecticut; the [2]Department of Internal Medicine, Yale University School of Medicine, New Haven, Connecticut; the [3]Department of Biomedical Engineering, Yale University School of Medicine, New Haven, Connecticut; the [4]Department of Cellular and Molecular Physiology, Yale University School of Medicine, New Haven, Connecticut; and the [5]Howard Hughes Medical Institute, Yale University School of Medicine, New Haven, Connecticut.

Corresponding author: Douglas E. Befroy, douglas.befroy@yale.edu.

Received 30 April 2012 and accepted 11 July 2012.

DOI: 10.2337/db12-0558

See accompanying review, Diabetes 2012;61:1927–1934.

THE MT TECHNIQUE

The MT techniques work on the principle that if the MR signal of an exchanging metabolite is perturbed, the transfer of this effect to its exchange partner can be detected, while leaving the underlying chemical equilibrium unaffected. The perturbation may either eliminate (saturate) or invert the signal of the initial metabolite of interest and is accomplished by applying a frequency-selective saturation or inversion pulse prior to acquiring the MR spectrum. These approaches give rise to the saturation-transfer (ST) and inversion-transfer techniques, respectively. For in vivo studies, the ST technique is typically used because of ease of calibration of an effective frequency-selective saturation pulse. On in vivo MR systems, particularly those used for human studies, the accurate, short-duration inversion pulses required for the inversion-transfer technique are difficult to implement due to inherent limitations in radiofrequency field homogeneity and the high-power requirements of such pulses. The ST effect from the terminal (γ) phosphate group of ATP to PCr due to the CK equilibrium and to P_i due to ATP synthesis/hydrolysis in skeletal muscle is shown in the ^{31}P spectra in Fig. 1. The magnitude of the effect (e.g., ΔPCr or ΔP_i) is proportional to the kinetics of exchange. Underlying assumptions for the application of the technique are that the metabolites of interest have distinct peaks in the MR spectrum, that exchange is at steady state (i.e., that the metabolite concentrations do not change during the experiment), and that exchange is rapid with respect to the lifetime of the MR signal.

The ATP synthesis/hydrolysis cycle is a phosphate-exchange reaction under the chemical equilibrium shown in Eq. 1, where k_f and k_r are the forward and reverse

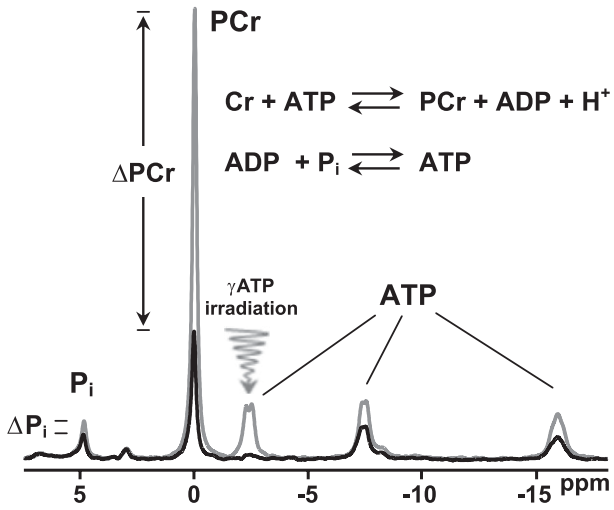

FIG. 1. The ^{31}P-ST technique can be applied in human muscle in vivo to assess the unidirectional fluxes that contribute to phosphate-exchange reactions. Irradiating the γATP peak with a frequency-selective saturation pulse leads to a reduction in the phosphocreatine (ΔPCr) and inorganic phosphate (ΔP_i) signals due to phosphate exchange via CK or the ATP synthesis/hydrolysis cycle.

rate constants. From simple reaction kinetics, the forward reaction ($P_i \rightarrow$ ATP flux) rate is equivalent to the forward rate constant multiplied by the concentrations of ADP and P_i (Eq. 2). At steady state, the tissue concentration of ADP remains constant, and this relationship can be simplified to generate a pseudo–first-order rate constant of exchange for P_i (k'_f) that incorporates the effects of the ADP concentration (Eq. 3). During the ST experiment (Fig. 1), γATP saturation causes a reduction in the observed P_i signal (M') from its equilibrium value (M_0) due to the effects of phosphate exchange (i.e., k'_f) and the influence of the effective MR relaxation time (T_1') of P_i (Eq. 4).

$$\mathrm{ADP} + \mathrm{P_i} \underset{k_r}{\overset{k_f}{\rightleftharpoons}} \mathrm{ATP} \qquad \text{Eq (1)}$$

$$V_{\mathrm{Pi}\rightarrow\mathrm{ATP}} = k_f[\mathrm{ADP}][\mathrm{P_i}] \qquad \text{Eq (2)}$$

$$V_{\mathrm{Pi}\rightarrow\mathrm{ATP}} = k'_f[\mathrm{P_i}] \qquad \text{Eq (3)}$$

$$k'_f = (1 - M'/M_0)/T_1' \qquad \text{Eq (4)}$$

Equation 4 requires that the following conditions are met: that there is full equilibration between the sites of ATP utilization (i.e., in the cytosol) and ATP production (mitochondria and cytosol); that across this system, ATP production ≡ utilization; that the saturation pulse fully nulls the γATP signal and has minimal off-resonance effects; and that the detected compartment (i.e., cytosolic P_i) is fully MR-visible and not participating in competing reactions. A more detailed description of the effects of chemical exchange on the observed MR signal and the derivation of these equations is beyond the scope of this article but can be found in the classic articles describing MT from McConnell (1) and Forsen and Hoffman (2).

From a practical perspective, the estimation of $P_i \rightarrow$ ATP flux therefore requires the determination of three parameters: *1*) calculation of the ST effect (M'/M_0) from γATP to P_i; *2*) calibration of the T_1 of P_i under conditions of γ-ATP saturation (T_1'); and *3*) determination of the intracellular P_i concentration. The unidirectional ($P_i \rightarrow$ ATP) flux that contributes to the exchange can then be calculated according to Eq. 3. To ensure that a study is fully described, we recommend that all of these parameters are reported when publishing data acquired using the ^{31}P-ST technique. Two experimental approaches are possible: in the progressive saturation experiment, M' and T_1' are determined simultaneously by acquiring a series of spectra in which the duration of the saturation pulse is gradually lengthened, and the extent of the ST effect increases until steady state is achieved. Alternatively, M' can be determined from a single spectrum in which the duration of the saturation pulse is sufficient (i.e., several times T_1') to establish the new steady-state MR equilibrium, with T_1' determined by a separate experiment. An inversion-recovery calibration with γATP saturation during the repetition time (T_R) and throughout the inversion delay will typically be performed to estimate T_1'. The intracellular concentration of P_i can be determined from a fully relaxed ^{31}P spectrum (where $T_R >> T_1$, and all metabolites are detected with equal sensitivity) with reference to ATP as an internal standard. Imperfections in the frequency specificity of the saturation pulse can lead to off-resonance effects modulating the intensity of the peak of interest. Therefore, M_0 is usually determined under control saturation conditions with the saturation pulse irradiating a downfield frequency from P_i that mirrors the separation between the γATP and P_i peaks. These effects can be significant, particularly at lower MR field strengths in which the frequency separation between the exchanging metabolites is relatively small (3,4). The performance and off-resonance effects of a saturation pulse are also influenced by its duration and therefore may not be consistent between the variable saturation pulse lengths of the progressive saturation experiment. We have found that this tends to lead to an underestimate of T_1' and prefer the steady-state style experiment, in which pulse performance is equivalent among all scans.

PRACTICAL CONSIDERATIONS FOR THE IMPLEMENTATION OF ^{31}P-ST IN VIVO

Because rates of $P_i \rightarrow$ ATP flux determined using the ^{31}P-ST experiment incorporate the measurement of three independent parameters (M'/M_0, T_1', and $[P_i]$), it is important to estimate these parameters as accurately as possible. High signal/noise ^{31}P spectra are required, particularly for the determination of M'/M_0, in which a relatively small decrement (~20%) in the magnitude of the P_i resonance, present in relatively low concentration (~2 mmol/L) compared with the other ^{31}P metabolites, is detected. Therefore, a stable experimental setup is required that minimizes or eliminates movement of the region of interest. Inadvertent contractions may perturb the maintenance of metabolic steady state in muscle and should be prevented. For animal experiments, these conditions are best satisfied by performing the ST experiment under light anesthesia. To ensure precision in the estimate of M'/M_0 in our studies, we repeat the measurement multiple times to confirm experimental stability.

The duration of the experiment will be dependent on the tissue of interest, species, and field strength of the MR system used. Our ^{31}P-ST experiments in human muscle take ~60 min on a 4 Tesla system, whereas 4–6 h are required for an ST experiment in mouse hindlimb at 9.4 Tesla due to the relatively small mass of muscle tissue available. The overall length of the ST experiment is dominated by the estimation of T_1', which requires the acquisition of several spectra to characterize the evolution of the MR signal. This

calibration can be shortened by obtaining fewer points, although this will also decrease the accuracy of the calibration. Faster methods are available that allow the estimation of T_1 by varying the extent to which the MR signal is excited (variable flip-angle methods) (5); however, the implementation of these methods in vivo can be problematic because very accurate excitation pulses are required for precise estimation of the T_1 relaxation time.

BIOLOGICAL APPLICATIONS OF ^{31}P-ST TO MEASURE $P_I \rightarrow$ ATP FLUX

The biological feasibility of using the ST technique to assess $P_i \rightarrow$ ATP flux was initially demonstrated in cell suspensions of *Escherichia coli* (6). Subsequent experiments in yeast cell suspensions (7) and implementation of the technique in the isolated perfused heart (8,9) and perfused liver (10) preparations demonstrated the applicability of the technique in a variety of in vitro systems. Translation of the methodology to in vivo applications was first performed in rat brain (11) followed by studies in the exercising rat hindlimb in vivo (12) and semi-invasive studies of dog (13) and lamb heart (14). We sought to add in vivo estimates of $P_i \rightarrow$ ATP flux by ^{31}P-ST to complement ^{13}C-MRS methods we were developing to assess rates of substrate oxidation via the tricarboxylic acid cycle (TCA cycle flux) in resting skeletal muscle. We initially performed proof-of-principle studies in rat hindlimb (15,16) followed by studies in human muscle to validate the methods (17) and examine how these metabolic fluxes were modulated by aging (18), insulin resistance (19,20), and endurance exercise training (21). We have also taken advantage of transgenic mouse models to examine how overt genetic modulations of mitochondrial content (22) and metabolism may influence the flux measured by the ^{31}P-ST technique (23; D.E.B. and G.I.S., unpublished observations). More recently, there has been a rapid expansion in the number of studies using the ^{31}P-ST technique in vivo, with applications examining the effects of insulin stimulation (24,25), insulin resistance (26–28), diabetes (29,30), MELAS (mitochondrial encephalopathy, lactic acidosis, and stroke-like episodes) syndrome (31), and acromegaly (32) on resting muscle $P_i \rightarrow$ ATP flux. Pilot studies have been reported in human liver (33,34), and validation experiments have been performed in human (35,36) and rat (37) brain.

LIMITATIONS OF THE ^{31}P-ST TECHNIQUE

The early studies examining the applications of the ^{31}P-ST technique in vitro observed that under certain conditions, the measured $P_i \rightarrow$ ATP flux was significantly greater than that predicted from oxygen consumption measurements, assuming the theoretical phosphate-to-oxygen (P:O) ratio for mitochondrial oxidative phosphorylation of ~3. This phenomenon was demonstrated not only in yeast (7,38) but also in isolated perfused heart (39) and liver (10). The study by Alger et al. (7) noted that an appreciable $P_i \rightarrow$ ATP flux could be detected in yeast under anaerobic conditions that was insensitive to the mitochondrial inhibitor oligomycin, suggesting that ATP synthesis via glycolysis was also detected by ^{31}P-ST and may augment the flux observed under aerobic conditions. Studies using glyceraldehyde-3-phosphate dehydrogenase (GAPDH) and phosphoglycerate kinase (PGK) in solution at concentrations and conditions designed to mimic those found in the Langendorff perfused heart confirmed that these enzymes could catalyze a significant $P_i \rightarrow$ ATP flux (40). Subsequent experiments using iodoacetate to inhibit ATP generation via the GAPDH/PGK enzyme couple demonstrated that these enzymes were contributing significantly to the measured $P_i \rightarrow$ ATP flux rates in these systems (10,38,39) potentially via catalyzing $P_i \leftrightarrows$ ATP exchange. With the GAPDH/PGK contribution eliminated, the apparent P:O ratio was normalized to ~2 to 3, below the theoretical limit (38,39). It has also been demonstrated using radiolabeled phosphate that near equilibrium $P_i \leftrightarrows$ ATP exchange can occur within isolated mitochondria at low respiration rates (41), either at the level of the ATP synthase complex or the adenine-nucleotide translocase (ANT). At higher respiration rates, the reverse flux (ATP $\rightarrow P_i$) was significantly decreased, leading to a switch from reversible $P_i \leftrightarrows$ ATP exchange to unidirectional ATP production by the mitochondrion. This observation is consistent with the normalization of P:O at higher workloads in heart (14,39) and exercising rat muscle in vivo (12). Overexpression of the F_1F_0 ATP synthase in *E. coli* had no effect on the $P_i \rightarrow$ ATP flux measured by ^{31}P-ST (42) under aerobic conditions. In contrast, overexpression of the ANT in yeast oxidizing glucose led to a significant increase in $P_i \rightarrow$ ATP flux (43), indicating a role for the ANT in catalyzing $P_i \leftrightarrows$ ATP exchange.

INFLUENCE OF NEAR-EQUILIBRIUM $P_i \leftrightarrows$ ATP EXCHANGE ON IN VIVO STUDIES USING ^{31}P-ST

Recent articles have expressed concern over the contribution of unidentified $P_i \leftrightarrows$ ATP exchange mechanisms to absolute rates of $P_i \rightarrow$ ATP flux measured in vivo using ^{31}P-ST, highlighting the discrepancy between estimated P:O ratios and querying whether this unidirectional flux reflects mitochondrial activity (44–46). In addition to putative contributions from exchange via GAPDH/PGK (45) and at the mitochondrion, Balaban and Koretsky (46) suggest that small metabolite pools, undetectable in the ^{31}P-MR spectrum due to their low concentration, could be irradiated during the ST experiment, undergo exchange with P_i, and contribute to the observed MT effect. These concerns are certainly valid in terms of deconvoluting the specific mechanisms that contribute to the $P_i \rightarrow$ ATP flux and quantifying absolute rates of net (i.e., forward flux minus reverse flux) mitochondrial ATP synthesis.

When considering the extent to which glycolytic ATP production or GAPDH/PGK exchange may contribute to the observed rates of $P_i \rightarrow$ ATP flux measured by the ^{31}P-ST experiment in vivo, it is worth noting that observations from these in vitro studies may not translate directly to those in an intact organisms due to several factors. Firstly, absolute rates of $P_i \rightarrow$ ATP flux measured in vitro in both cell preparations and isolated organs are significantly higher than those measured in vivo (Table 1). These in vitro systems are often studied under conditions in which glucose is the sole or primary substrate, which may enhance the contribution of glycolytic metabolism to the measured $P_i \rightarrow$ ATP flux and play a role in the erroneously high P:O ratios observed in these preparations. Furthermore, there are substantial differences in the expression of glycolytic enzymes between tissues and different species. The expression/activity levels for PGK, which exhibits a high flux control coefficient for ATP $\leftrightarrows P_i$ exchange (47), can vary by an order of magnitude among human tissues and between the same tissue in humans and rodents (Table 2). Resting skeletal muscle, for example, derives most of its energy from fat oxidation rather than glycolysis, and this is reflected in the relative PGK activity where heart $\approx$ brain $>>$ liver $>$ muscle. PGK activity in most human tissues is significantly lower than in the counterpart tissue in rats and substantially

TABLE 1
Absolute $P_i \rightarrow ATP$ flux rates reported in the literature for different in vitro and in vivo preparations

Reference	Tissue	Reported $P_i \rightarrow ATP$ flux	Equivalent flux (μmol/g/min)
Alger et al. (7)	Yeast cell suspension	3.5 ± 1 μmol/g (cells)/s	210 ± 60
Campbell-Burk et al. (38)	Yeast cell suspension	1.8 ± 0.5 μmol/g (cells)/s	108 ± 30
Matthews et al. (8)	Isolated rat heart	2.8 ± 0.3 μmol/g (cells)/s	32 ± 3.5*
Kingsley-Hickman et al. (39)	Isolated rat heart	7.1 ± 0.8 μmol/g (cells)/s	82 ± 9.2*
Robitaille et al. (13)	Dog heart in vivo (postischemic)	0.41± 0.09 μmol/g/s	24.6 ± 5.4
Portman (14)	Sheep heart in vivo (low workload)	81± 4 μmol/g/min	81 ± 4
Thoma and Uğurbil (10)	Perfused rat liver	4.26 ± 0.27 μmol/g (dw)/min	64 ± 4†
Schmid et al. (34)	Human liver in vivo	29.5± 1.8 mmol/L/min	28 ± 1.7‡
Brindle et al. (12)	Rat muscle in vivo (resting)	0.8 μmol/g (dw)/s	11.0§
Brindle et al. (12)	Rat muscle in vivo (stimulated)	2.5 ± 0.5 μmol/g (dw)/s	35 ± 6.9§
Jucker et al. (16)	Rat muscle in vivo (resting)	83 ± 14 nmol/g/s	4.98 ± 0.84
van den Broek et al. (90)	Rat muscle in vivo	8.33 ± 1.53 μmol/g/min	8.33 ± 1.53
Choi et al. (22)	Mouse muscle in vivo	4.73 ± 0.56 μmol/g/min	4.73 ± 0.56
Petersen et al. (18)	Human muscle in vivo	7.50 ± 0.77 μmol/g/min	7.50 ± 0.77
Schmid et al. (101)	Human muscle in vivo	0.234 ± 0.043 mmol/L/s	9.42 ± 1.73‖
Du et al. (37)	Rat brain in vivo	12.1 ± 1.9 μmol/g/min	12.1 ± 1.9
Shoubridge et al. (11)	Rat brain in vivo	0.33 μmol/g/s	19.8
Du et al. (36)	Human brain in vivo (occipital lobe)	8.8 ± 1.9 μmol/g/min	8.8 ± 1.9
Lei et al. (35)	Human brain in vivo (visual cortex)	12.1 ± 2.8 μmol/g/min	12.1 ± 2.8

*Assumed wet weight/dry weight (dw) = 5.20 (102). †Reported wet weight/dry weight (dw) = 4.00. ‡Assumed liver density = 1.05 g/mL (103). §Reported wet weight/dry weight (dw) = 4.35. ‖Assumes 8.2 mmol ATP ≡ 5.5 μmol/g (104).

lower than that in mice, reflecting the greater reliance on glycolytic metabolism in rodents. In brain, despite the high PGK activity and significant role for glycolysis, close to theoretical P:O ratios have been reported (35,37). The extrapolation of metabolic mechanisms between in vitro and in vivo preparations, from one tissue to another or between different species, is therefore not straightforward, and we urge caution when interpreting the ramifications of an observation in a particular preparation.

In the following section, we will describe our experiences with the ^{31}P-ST technique in a variety of systems, which along with studies from other laboratories, support the notion that $P_i \rightarrow ATP$ flux responds to perturbations in oxidative metabolism and, when supported by complementary methods, can be used as a biomarker of in vivo mitochondrial activity. Detailed descriptions of the experimental procedures we have used can be found in the cited literature. It is worth noting that although different MR systems were used, we implemented comparable ^{31}P-ST protocols for all of our human and rodent studies. Saturation-pulse lengths, sequence repetition times, and the delays for the inversion-recovery calibration were optimized according to the inherent T_1' of P_i on each MR system, and appropriate coil geometries were chosen for the region of interest.

The most compelling evidence we have obtained that demonstrates that the $P_i \rightarrow ATP$ flux measured by ^{31}P-ST responds to perturbations in skeletal muscle oxidative function is from transgenic mouse models with direct manipulation of genes that modulate mitochondrial content and metabolism. Mice with muscle-specific overexpression of peroxisome proliferator–activated receptor γ (PPARγ) coactivator 1α (PGC1α), a regulator of oxidative metabolism, exhibit increased mitochondrial density and enhanced expression and protein content of genes involved in oxidative phosphorylation. $P_i \rightarrow ATP$ flux in the muscle of these mice was increased ~40% (Fig. 2), and a concomitant increase in fatty-acid oxidation was detected in isolated soleus muscle strips (22). It is interesting to note that short-term (3 weeks) high-fat feeding enhanced muscle $P_i \rightarrow ATP$ flux in both wild-type and PGC1α overexpressing mice (22) (Fig. 3). This phenomenon is supported by data obtained from rats fed a high-fat diet for 2.5 weeks in which the in vivo oxidative capacity of muscle (assessed using the ^{31}P-MRS PCr recovery method) was increased as well as mitochondrial DNA content and the oxidative capacity of isolated mitochondria (48), presumably to increase the ability to oxidize the excess of available lipid. Significantly, this enhancement in mitochondrial capacity had dissipated after 25 weeks of high-fat feeding, despite a sustained elevation in mitochondrial DNA, which corresponds with the decreased muscle $P_i \rightarrow ATP$ flux observed in rats fed a high-fat diet for longer (10-week) duration (49). Uncoupling protein 3 (UCP3) is a mitochondrial membrane protein found in skeletal muscle that has high homology with UCP1, which is found in brown adipose tissue and mediates thermogenesis by dissipating the H^+ electrochemical gradient across the inner mitochondrial membrane. We observed that in vivo skeletal muscle $P_i \rightarrow ATP$ flux was increased in UCP3 knockout mice (23); conversely, muscle-specific overexpression of UCP3 led to a decreased flux (D.E.B. and G.I.S., unpublished observations) [Fig. 2, data were acquired using the same MR protocols as described in Choi et al. (22)]. These observations are supported by in vitro data. The ATP/ADP ratio was increased in mitochondria isolated from the muscle of UCP3-knockout mice, and State III (ADP-stimulated) respiration rates were increased (50). Palmitate and pyruvate oxidation have been observed to be elevated in soleus

TABLE 2
Protein expression/activity (arbitrary units) of PGK1 isoform between different tissues and species

PGK1	Muscle	Heart	Liver	Brain
Human	34	304	65	~460
Rat	2,875	1,405	—	~1,000
Mouse	9,856	6,191	4,143	~3,700

Data courtesy of the BioGPS gene portal (www.biogps.org).

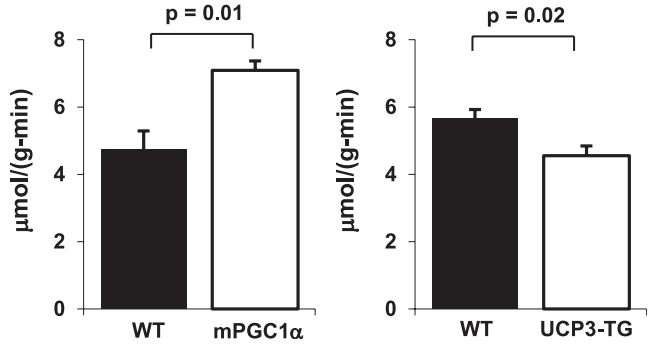

FIG. 2. Direct manipulation of genes involved in mitochondrial content and metabolism modulates muscle $P_i \rightarrow ATP$ flux. Mice with muscle-specific overexpression of PGC1α (mPGC1α), a regulator of oxidative metabolism that increases mitochondrial density and enhances expression and protein content of genes involved in oxidative phosphorylation, exhibit a concomitant increase in $P_i \rightarrow ATP$ flux compared with wild-type (WT) mice. Muscle $P_i \rightarrow ATP$ flux is decreased in transgenic mice that overexpress UCP3 (UCP3-TG, D.E.B. and G.I.S unpublished observations), a mitochondrial membrane protein found in skeletal muscle that may uncouple the H^+ electrochemical gradient across the inner mitochondrial membrane and decrease the efficiency of oxidative phosphorylation. Data obtained from UCP3-TG mice were acquired using the same experimental protocols described in Choi et al. (22). Data adapted from Choi et al. (22), reproduced courtesy of the National Academy of Sciences.

muscle strips isolated from UCP3 overexpressing mice (51) accompanied by an increased in State IV (nonstimulated) respiration rates in mitochondria (52) and whole-body energy expenditure (53).

To more fully characterize mitochondrial oxidative function in skeletal muscle in vivo, we use estimates of $P_i \rightarrow ATP$ flux assessed by ^{31}P-ST in conjunction with direct measurements of substrate oxidation via the TCA cycle using dynamic ^{13}C-MRS. A thorough analysis of this technique is beyond the scope of this article and can be found in the literature (20,54), but a brief description is warranted. Rates of TCA cycle flux in muscle can be estimated by infusing ^{13}C-labeled acetate and using ^{13}C-MRS to monitor ^{13}C-label incorporation into the muscle glutamate pool, which acts as a surrogate for the intermediates of the TCA cycle. Kinetic analysis of the time courses of ^{13}C glutamate enrichment can be accomplished using computer-modeling techniques to fit the data to a metabolic model of the TCA cycle, and rates of acetate oxidation and total TCA cycle flux can be estimated. These studies use pharmacy-prepared, sterile infusates of acetate, a naturally occurring endogenous substrate, that have been positionally enriched with the MR-visible stable isotope of carbon (^{13}C). Concentrations of plasma acetate during the infusion remain relatively low (~1 mmol/L) to avoid mass action effects of the substrate that could otherwise influence metabolism. As such, these studies can be accomplished under conditions that minimize the perturbation of resting muscle metabolism, are minimally invasive, and very safe.

We found that both $P_i \rightarrow ATP$ flux, measured by ^{31}P-ST, and TCA cycle flux, measured by ^{13}C-MRS, were both reduced by ~40% in the calf muscles of healthy, lean, elderly individuals (~70 years of age) with respect to healthy, young (~27 years), control subjects who were matched for BMI and physical activity (Fig. 4) (18). Similarly, using the same ^{13}C- and ^{31}P-MRS methods, both TCA cycle and $P_i \rightarrow ATP$ flux were reduced by ~30% in healthy, young, lean, insulin-resistant (IR) offspring of type 2 diabetic patients (IR offspring) compared with age-BMI-activity–matched insulin-sensitive (IS) control subjects (IS subjects) (19,20) (Fig. 5). In vitro analysis of muscle biopsy samples from a similar cohort of IR offspring (55) revealed a comparable ~35% reduction in mitochondrial density, as assessed by electron microscopy, as well as decreased content of proteins associated with oxidative phosphorylation (cytochrome *c* oxidase-1, succinate dehydrogenase, and pyruvate dehydrogenase) compared with matched IS subjects. This reduction in mitochondrial content and function in the young, lean IR offspring was consistent with a reduction in the ratio of slow-twitch (oxidative) muscle fibers to fast-twitch (glycolytic) fibers (19).

We have also examined muscle-specific $P_i \rightarrow ATP$ flux in different muscle groups of the calf using a localized version of the ^{31}P-ST method to restrict the measurement to either the gastrocnemius or soleus muscle compartments (Fig. 6). Muscle-specific $P_i \rightarrow ATP$ flux, measured in healthy volunteers, was significantly faster in the soleus muscle compared with the gastrocnemius ($V_{Pi \rightarrow ATP}$ = 8.12 ± 0.86 vs. 4.97 ± 1.08 mmol/g/min) (56). This disparity in $P_i \rightarrow ATP$ flux is consistent with the differences in mitochondrial number, oxidative enzyme content, and oxygen consumption expected for the more oxidative phenotype of the soleus than the gastrocnemius (57–61).

We have used the combination of ^{31}P-ST assessment of $P_i \rightarrow ATP$ flux and ^{13}C-MRS measurement of TCA cycle flux to noninvasively assess energetic efficiency in skeletal

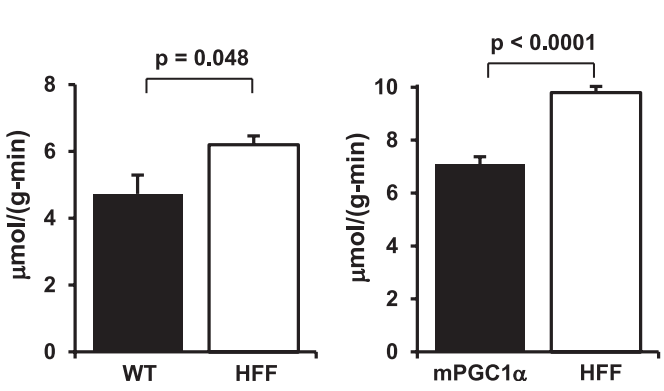

FIG. 3. Three weeks of high-fat feeding (HFF) in both wild-type (WT) mice and mice with muscle-specific overexpression of PGC1α (mPGC1α) leads to an increase in muscle $P_i \rightarrow ATP$ flux. Data reproduced from Choi et al. (22), courtesy of the National Academy of Sciences.

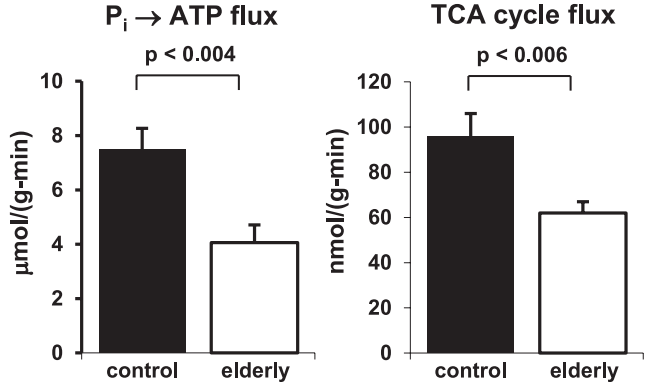

FIG. 4. Both $P_i \rightarrow ATP$ flux, assessed by ^{31}P-ST MRS, and TCA cycle flux, measured using ^{13}C-MRS to monitor the metabolism of infused [2-^{13}C] acetate, were reduced by ~40% in the muscle of healthy elderly subjects. Data adapted from Petersen et al. (18), reproduced courtesy of *Science*.

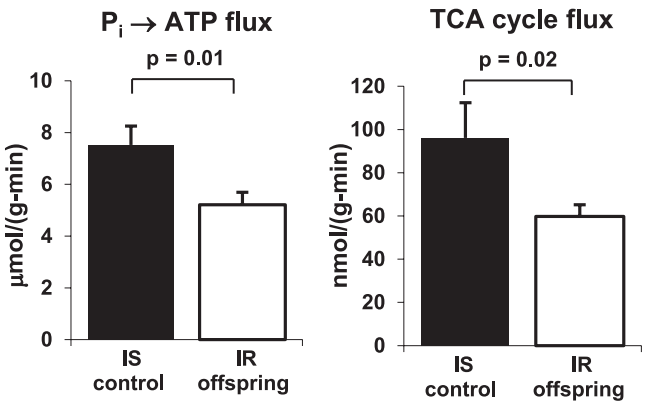

FIG. 5. $P_i \rightarrow$ ATP flux was reduced by ~30% in healthy, young, lean IR offspring of type 2 diabetic patients (IR offspring) compared with age-BMI-activity–matched IS control subjects (IS subjects). A similar decrease in TCA cycle flux was observed in an equivalent group of IR offspring. Adapted from Petersen et al. (19) and reproduced courtesy of the *New England Journal of Medicine*. Data reproduced from Befroy et al. (20).

muscle in both humans and rodents (16,17). Mitochondrial uncoupling stimulated by acute 2,4-dinitrophenol (DNP) or chronic thyroid hormone (T3) administration are known to lead to an increase in oxygen consumption (16,62–66). Consistent with this mechanism of action, DNP and T3 treatment in rats caused substantial increases in muscle TCA cycle flux, yet the $P_i \rightarrow$ ATP flux was unaffected, reflecting decreased mitochondrial efficiency (16). This observation was supported by a lack of effect of either T3 or DNP on the ATPase activity of isolated mitochondria or any detectable differences in muscle GAPDH/PGK exchange rates assessed by the deuterated glucose technique. Similar decreases in mitochondrial energetic efficiency using the same in vivo ^{13}C-/^{31}P-MRS methods have also been observed in human skeletal muscle in response to T3 treatment (17).

These data indicate that rates of resting muscle $P_i \rightarrow$ ATP flux and substrate oxidation via the TCA cycle determined using ^{31}P- and ^{13}C-MRS techniques appear to track qualitatively with modulations in mitochondrial content and the extent of mitochondrial uncoupling. Assuming that three molecules of O_2 are ultimately consumed per C_2 unit oxidized by the TCA cycle and that the P:O ratio is ~3 (these approximations hold whether the substrate source is fatty acids or glucose), rates of muscle $P_i \rightarrow$ ATP flux are estimated to be ~1.6 μmol/g/min. Therefore, absolute rates of ATP production measured using the ^{31}P-ST technique (~7.5 μmol/g/min) are still significantly higher than those calculated from TCA cycle activity. It is worth noting that this discrepancy in ATP production (~4.7-fold) is far lower than that estimated from measurements of oxygen consumption by arterio/venous (A/V) difference, near infrared spectroscopy (NIRS), and $^{15}O_2$ positron emission tomography (44). This is because rates of oxygen consumption calculated from TCA cycle flux data (~0.29 μmol(O_2)/g/min) exceed those calculated by NIRS and positron emission tomography by 3–10-fold and are at the upper limit of literature values reported using A/V difference methods. We believe that phenotypic differences in the muscle group(s) examined using the different techniques contribute, in part, to these discrepancies in rates of O_2 consumption and may be exacerbated by experimental considerations for each method. For example, A/V difference methods tend to sample blood-oxygen concentration across an entire limb in which other tissues may contribute to the measured O_2 consumption. Accurate estimates of muscle mass/volume are also required to determination rates of O_2 utilization. NIRS techniques sample from a relatively superficial region of interest that may not exhibit comparable rates of O_2 consumption to the bulk of the tissue. We feel that the most relevant methodological comparison is between the TCA cycle flux and ^{31}P-ST because both ^{13}C and ^{31}P data were acquired from comparable regions of interest in the calf muscles. As discussed above, we believe that the disparity in absolute rates of ATP production estimated by these methods in resting muscle is likely because of near equilibrium $P_i \leftrightarrows$ ATP exchange at the level of the mitochondria, with only a minor contribution from exchange catalyzed by GAPDH/PGK.

Data from other groups also support the notion that in vivo estimates of $P_i \rightarrow$ ATP flux correlate with tissue oxidative metabolism. Brindle et al. (12) examined the effects of electrically stimulated contractions on rat muscle using ^{31}P-ST and observed a linear response of $P_i \rightarrow$ ATP flux to increases in muscle workload. An earlier study in perfused muscle established that muscle oxygen consumption is also proportional to workload (67). Comparing the data from these studies, despite $P_i \leftrightarrows$ ATP exchange contributing to the measured unidirectional $P_i \rightarrow$ ATP flux at rest and leading to an overestimation in the P:O ratio in quiescent muscle, at higher workloads the P:O ratio trended toward the theoretical value. Although the increases in $P_i \rightarrow$ ATP flux and oxygen consumption due to muscle contraction were not directly proportional, the ^{31}P-ST measurement appeared to track oxygen utilization and therefore respond to increases in mitochondrial activity. In the rat brain, by modulating the depth of anesthesia, $P_i \rightarrow$ ATP flux was

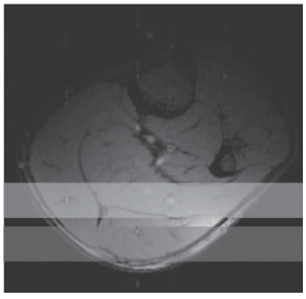

	Gastrocnemius (n = 5)	Soleus (n = 5)
M' / M_0	0.86 ± 0.04	0.77 ± 0.03
T_1' (sec^{-1})	2.47 ± 0.23	3.90 ± 0.19 *
k' (sec^{-1})	0.057 ± 0.012	0.059 ± 0.007
$[P_i]$ (μmol/g)	1.45 ± 0.09	2.35 ± 0.21 *
$P_i \rightarrow$ ATP μmol/(g-min)	4.97 ± 1.08	8.12 ± 0.86 *

* $P < 0.05$

FIG. 6. Muscle-specific rates of $P_i \rightarrow$ ATP flux were obtained using a localized ^{31}P-ST pulse-sequence to restrict detection to either the gastrocnemius or soleus muscles of the calf. Estimated rates for each muscle compartment are noted in the table.

found to be tightly correlated with the cerebral activity level and the extent of energy demand (37). Similarly, rates of $P_i \rightarrow ATP$ flux measured in the human visual cortex (35) and monkey brain (68) agree well with predicted values calculated from cerebral metabolic rates of glucose or oxygen consumption or from MRS measurements of TCA cycle flux.

METABOLIC IMPLICATIONS OF DIFFERENCES IN RESTING MUSCLE $P_i \rightarrow ATP$ FLUX

In contracting muscle, numerous studies have demonstrated that mitochondrial ATP production is likely to be demand-driven and regulated through substrate-level feedback via ADP and P_i, both of which increase in response to contractile activity. The factors that regulate mitochondrial activity in resting muscle in vivo are less clear, in which any underlying metabolic perturbations are likely to be more subtle (and therefore difficult to detect experimentally). In this section, we discuss the metabolic implications that stem from our observations of reduced rates of basal $P_i \rightarrow ATP$ flux in the muscle of elderly individuals and IR offspring.

Under basal conditions, protein synthesis and the maintenance of ion homeostasis are likely to be the major cellular processes that consume ATP. There is evidence to suggest that rates of protein synthesis are decreased in the muscle of elderly subjects (69,70) and that pH and ion homeostasis may be disrupted (71,72). Although blunted increases in protein synthesis in response to insulin stimulation have been reported in individuals with type 2 diabetes (73), basal rates of muscle protein synthesis appear to be unaffected (74). Decreased content and activity of the Na^+/K^+-ATPase, a transmembrane ion pump that maintains the cellular membrane homeostasis, has been reported in type 2 diabetic patients (75), obese IR individuals (76), and in response to high-fat feeding (77). The activity of this protein may contribute significantly to basal energy requirements in muscle as well as other tissues (78). These observations match with the decreases in TCA cycle and ATP flux that we observe in the muscle of elderly and IR offspring; however, the implication of cause and effect is unclear. Although a mechanism of demand-driven regulation of resting ATP flux is plausible, it is also feasible that protein synthesis may have been downregulated and/or ion homeostasis disrupted due to the decreased availability of ATP.

Interestingly, under resting conditions in which intracellular concentrations of both ADP and P_i are low, it has been suggested that the cellular redox potential (i.e., availability of NADH) may also exert respiratory control (79,80). Our observations of decreased $P_i \rightarrow ATP$ flux in the muscle of elderly and IR individuals may be a result of the decreased TCA cycle activity, which reduces the availability of NADH for oxidation by the electron transport chain.

A recent study by Lim et al. (30) has suggested that the decreased rates of muscle ATP turnover observed in type 2 diabetic subjects may be due to reduced rates of glucose uptake and glycogen synthesis. We do not believe that such effects are likely to play a significant role in our studies of the elderly or IR offspring because glucose disposal in resting muscle under fasting conditions will be very low and of insufficient magnitude to exert an effect on oxidative rates.

COMPARISON OF ^{31}P-ST WITH OTHER METHODS FOR ESTIMATING IN VIVO MITOCHONDRIAL METABOLISM IN SKELETAL MUSCLE

As described above, we have implemented ^{31}P-ST measurements of $P_i \rightarrow ATP$ flux in conjunction with ^{13}C-MRS estimates of TCA cycle flux to assess muscle mitochondrial metabolism in vivo. Other groups have complemented their ^{31}P-ST measurements with dynamic ^{31}P-MRS to estimate muscle mitochondrial oxidative capacity from the kinetics of PCr repletion following a bout of exercise, a method that has been validated in humans and rat models (81). This functional estimate of oxidative capacity has been shown to correlate well with whole-body maximal oxygen consumption ($V_{O_{2max}}$) and estimates of mitochondrial capacity, enzyme expression/content and respiratory function of isolated mitochondria, determined in vitro using biopsy samples (82–85). Muscle oxidative capacity determined by PCr recovery has been demonstrated to be reduced in type 2 diabetic patients (86,87), although this finding is not universal (88,89). Interestingly, in a rat model of mitochondrial dysfunction, induced by chronic inhibition of complex 1 of the electron transport chain, hindlimb muscle oxidative capacity determined by PCr recovery was significantly decreased, whereas resting $P_i \rightarrow ATP$ flux was unaffected (90). Similarly, in human subjects with a genetic defect in insulin-receptor signaling, oxidative capacity of the vastus lateralis was decreased versus healthy controls, whereas resting $P_i \rightarrow ATP$ in the calf muscle was unchanged (26). However, it is unclear whether valid comparisons of the methods can be made in this study because each technique was performed in different muscle compartments where the metabolic phenotype is likely to differ significantly. The disagreement between findings with PCr recovery and ^{31}P ST in these studies has been used to query the ST method and whether it reflects oxidative activity in skeletal muscle. However, an alternate interpretation, which we support, is that the two measurements assess different aspects of mitochondrial function: total muscle oxidative capacity versus resting energy production, that are not necessarily proportional due to intracellular regulation of mitochondrial function.

Although the PCr recovery method seems to provide an excellent estimate of functional mitochondrial/oxidative capacity, several factors concerning the effective application of the method should be considered for those unfamiliar with the technique. The kinetics of PCr repletion following exercise are usually characterized by fitting the recovery to a monoexponential and assuming the post-exercise ATP generation is entirely oxidative (91). However, bi- or multiexponential behavior has been observed in response to high-intensity exercise. This response may be a consequence of tissue heterogeneity or differences in fiber recruitment during exercise, although a contribution of glycolytic ATP production has also been suggested (92,93). Intracellular acidification, typically encountered during high-intensity exercise protocols, appears to slow the rate of PCr recovery potentially due to direct effects on mitochondrial respiration (94,95), the use of ATP for H^+ pumping to restore pH (84,96), or via modulating the CK equilibrium (97–99). The pH dependence of PCr recovery rates may also reflect selective recruitment of muscle fibers for low- versus high-intensity contractions (100).

The rate of muscle PCr depletion monitored by ^{31}P-MRS during limb ischemia induced by circulatory occlusion has also been used as an estimate of resting ATP use. A comparison of the ^{31}P-MRS methods has been performed in the calf muscles by Schmid et al. (101), who observed correlations among muscle $P_i \rightarrow ATP$ flux, the decline in PCr induced by cuff ischemia, and the time constant of PCr recovery (τ_{PCr}) following exercise protocol during ischemia. The correlation among these parameters would seem to suggest that each reflects oxidative activity;

however, we urge caution over the interpretation of these data due to methodological uncertainties in this study. Reservations include the lack of control over end-exercise pH, which, as described above, has been demonstrated to modulate the kinetics of PCr recovery, and the use of a plantar flexion exercise protocol in combination with a relatively large diameter coil for ^{31}P signal detection. Plantar flexion involves preferential activation of the gastrocnemius muscle groups, which will exhibit enhanced PCr depletion compared with the soleus and influence the observed PCr recovery kinetics. In contrast, the region of interest for the $P_i \rightarrow$ ATP flux and ischemic PCr utilization measurements performed in resting muscle will correspond to a weighted average of the soleus and gastrocnemius muscle groups. The relative contribution of deeper lying muscle groups in this study will be particularly exacerbated by the relatively large-diameter coil (10 cm) used for ^{31}P signal detection. The use of a smaller-diameter ^{31}P coil would act as a rudimentary method of signal localization by confining signal detection to the superficial muscle groups and ensure that the sampled volume was equivalent for each ^{31}P technique. Finally, we also have concerns over whether ischemic conditions are a valid metabolic environment in which to assess resting ATP turnover.

In vitro analyses of muscle biopsy samples may also offer additional insight into mitochondrial metabolism. Mitochondrial density, mitochondrial DNA copy number, the expression and content of mitochondrial proteins, as well as the respiratory function of isolated mitochondria or skinned muscle fibers provide a theoretical estimate of the maximal mitochondrial capacity and have been used as indirect markers of mitochondrial function. As mentioned above, the functional estimate of mitochondrial metabolism determined using the PCr recovery technique correlates with many of these theoretical estimates (82–85), reflecting that these methods are all biomarkers of mitochondrial capacity rather than resting or intermediate mitochondrial function. Taken together, these studies highlight that these techniques are likely measuring different aspects of mitochondrial metabolism, resting activity versus maximal capacity, and to more fully characterize the metabolic effects of an intervention or disease, multiple parameters of oxidative function, ideally a combination of resting function, maximal capacity, and the response to an intermediate metabolic demand, should be assessed.

Performing in vitro analyses of mitochondrial metabolism from muscle biopsy samples therefore enables an array of parameters to be assessed, and the experimental procedures involved are highly sensitive and can typically be accomplished in most laboratories. However, a number of caveats should be considered: the biopsy itself is an invasive measurement and is extracted from a small region of tissue that may not accurately represent the entire muscle. Repeated sampling, although feasible, will occur from slightly different regions of tissue that may not contain the same muscle fiber-type composition. The integrated network of metabolic processes that exist in vivo are no longer present, and assays usually provide an estimate of the theoretical maximal capacity without the limitations imposed by regulatory mechanisms, substrate availability, or product inhibition. Normalization of data can also be problematic because different internal reference standards (total protein content, total mitochondrial protein content, specific mitochondrial proteins) are often used. The MR methods described in this article offer the ability to estimate mitochondrial function in vivo, in which regulatory mechanisms remain intact and the same region of tissue can be sampled noninvasively and repeatedly, although this is obviously constrained by the availability of an MR system. The PCr recovery method is relatively straightforward to implement on many scanners and can yield estimates of functional muscle mitochondrial capacity, provided an appropriate contraction protocol is selected, particularly when studying populations that may have impaired muscle metabolism. The TCA cycle flux measurement using ^{13}C-MRS to monitor the oxidation of ^{13}C-labeled substrates is considerably more complex to implement and generally requires customized MR hardware/software as well as specialized metabolic modeling analyses. Additional constraints are provided by the length of the study (~2 to 3 h within the scanner), which may be prohibitive for certain subjects, and the overall cost of the experiment due to the need for ^{13}C-labeled substrates, extensive MR system time, and personnel. However, this method probably provides the most accurate estimate of resting mitochondrial activity in vivo.

CONCLUSION

In conclusion, MT MRS techniques offer a unique ability to examine the unidirectional fluxes that contribute to metabolic exchange reactions. The $P_i \rightarrow$ ATP flux associated with the ATP synthesis/hydrolysis cycle is of particular interest because it is a key bioenergetic process supporting the energy demands of a tissue. Although the ^{31}P-ST experiment measures all metabolic contributions to the $P_i \rightarrow$ ATP flux, including glycolytic ATP production and near-equilibrium exchange at the level of GAPDH/PGK and/or the mitochondrion, experiments in a variety of in vivo systems suggest that the flux does respond to perturbations in mitochondrial metabolism. Different experimental techniques to assess muscle metabolism in vivo (e.g. $P_i \rightarrow$ ATP flux by ^{31}P-ST, oxidative capacity by PCr recovery using dynamic ^{31}P-MRS, and substrate oxidation by dynamic ^{13}C-MRS) likely assess different parameters of mitochondrial function. Therefore, to more fully characterize oxidative function in vivo, we recommend the use of complementary analytical techniques to obtain a multiparametric assessment of mitochondrial metabolism.

ACKNOWLEDGMENTS

This work was supported by grants from the U.S. Public Health Service (R01-DK-49230, R01-DK-40936, R24-DK-085638, U24-DK-059635, P30-DK-45735, and R01-AG-23686) and a Distinguished Clinical Scientist Award (to K.F.P.) from the American Diabetes Association.

No potential conflicts of interest relevant to this article were reported.

D.E.B., D.L.R., K.F.P., and G.I.S. contributed to the writing of this article. D.E.B. is the guarantor of this work and, as such, had full access to all the data in the study and takes responsibility for the integrity of the data and the accuracy of the data analysis.

REFERENCES

1. McConnell HM. Reaction Rates by Nuclear Magnetic Resonance. J Chem Phys 1958;28:430–431
2. Forsen S, Hoffman RA. Study of Moderately Rapid Chemical Exchange Reactions by Means of Nuclear Magnetic Double Resonance. J Chem Phys 1963;39:2892–2901
3. Kingsley PB, Monahan WG. Effects of off-resonance irradiation, cross-relaxation, and chemical exchange on steady-state magnetization and effective spin-lattice relaxation times. J Magn Reson 2000;143:360–375

4. Kingsley PB, Monahan WG. Correcting for incomplete saturation and off-resonance effects in multiple-site saturation-transfer kinetic measurements. J Magn Reson 2000;146:100–109
5. Bottomley PA, Ouwerkerk R, Lee RF, Weiss RG. Four-angle saturation transfer (FAST) method for measuring creatine kinase reaction rates in vivo. Magn Reson Med 2002;47:850–863
6. Brown TR, Ugurbil K, Shulman RG. ^{31}P nuclear magnetic resonance measurements of ATPase kinetics in aerobic Escherichia coli cells. Proc Natl Acad Sci USA 1977;74:5551–5553
7. Alger JR, den Hollander JA, Shulman RG. In vivo phosphorus-31 nuclear magnetic resonance saturation transfer studies of adenosinetriphosphatase kinetics in Saccharomyces cerevisiae. Biochemistry 1982;21:2957–2963
8. Matthews PM, Bland JL, Gadian DG, Radda GK. The steady-state rate of ATP synthesis in the perfused rat heart measured by ^{31}P NMR saturation transfer. Biochem Biophys Res Commun 1981;103:1052–1059
9. Degani H, Laughlin M, Campbell S, Shulman RG. Kinetics of creatine kinase in heart: a ^{31}P NMR saturation- and inversion-transfer study. Biochemistry 1985;24:5510–5516
10. Thoma WJ, Uğurbil K. Saturation-transfer studies of ATP-Pi exchange in isolated perfused rat liver. Biochim Biophys Acta 1987;893:225–231
11. Shoubridge EA, Briggs RW, Radda GK. 31p NMR saturation transfer measurements of the steady state rates of creatine kinase and ATP synthetase in the rat brain. FEBS Lett 1982;140:289–292
12. Brindle KM, Blackledge MJ, Challiss RA, Radda GK. ^{31}P NMR magnetization-transfer measurements of ATP turnover during steady-state isometric muscle contraction in the rat hind limb in vivo. Biochemistry 1989;28:4887–4893
13. Robitaille PM, Merkle H, Sako E, et al. Measurement of ATP synthesis rates by ^{31}P-NMR spectroscopy in the intact myocardium in vivo. Magn Reson Med 1990;15:8–24
14. Portman MA. Measurement of unidirectional P(i)—>ATP flux in lamb myocardium in vivo. Biochim Biophys Acta 1994;1185:221–227
15. Jucker BM, Ren J, Dufour S, et al. ^{13}C/^{31}P NMR assessment of mitochondrial energy coupling in skeletal muscle of awake fed and fasted rats. Relationship with uncoupling protein 3 expression. J Biol Chem 2000;275:39279–39286
16. Jucker BM, Dufour S, Ren J, et al. Assessment of mitochondrial energy coupling in vivo by ^{13}C/^{31}P NMR. Proc Natl Acad Sci USA 2000;97:6880–6884
17. Lebon V, Dufour S, Petersen KF, et al. Effect of triiodothyronine on mitochondrial energy coupling in human skeletal muscle. J Clin Invest 2001;108:733–737
18. Petersen KF, Befroy D, Dufour S, et al. Mitochondrial dysfunction in the elderly: possible role in insulin resistance. Science 2003;300:1140–1142
19. Petersen KF, Dufour S, Befroy D, Garcia R, Shulman GI. Impaired mitochondrial activity in the insulin-resistant offspring of patients with type 2 diabetes. N Engl J Med 2004;350:664–671
20. Befroy DE, Petersen KF, Dufour S, et al. Impaired mitochondrial substrate oxidation in muscle of insulin-resistant offspring of type 2 diabetic patients. Diabetes 2007;56:1376–1381
21. Befroy DE, Petersen KF, Dufour S, Mason GF, Rothman DL, Shulman GI. Increased substrate oxidation and mitochondrial uncoupling in skeletal muscle of endurance-trained individuals. Proc Natl Acad Sci USA 2008;105:16701–16706
22. Choi CS, Befroy DE, Codella R, et al. Paradoxical effects of increased expression of PGC-1alpha on muscle mitochondrial function and insulin-stimulated muscle glucose metabolism. Proc Natl Acad Sci USA 2008;105:19926–19931
23. Cline GW, Vidal-Puig AJ, Dufour S, Cadman KS, Lowell BB, Shulman GI. In vivo effects of uncoupling protein-3 gene disruption on mitochondrial energy metabolism. J Biol Chem 2001;276:20240–20244
24. Petersen KF, Dufour S, Shulman GI. Decreased insulin-stimulated ATP synthesis and phosphate transport in muscle of insulin-resistant offspring of type 2 diabetic parents. PLoS Med 2005;2:e233
25. Lim EL, Hollingsworth KG, Thelwall PE, Taylor R. Measuring the acute effect of insulin infusion on ATP turnover rate in human skeletal muscle using phosphorus-31 magnetic resonance saturation transfer spectroscopy. NMR Biomed 2010;23:952–957
26. Sleigh A, Raymond-Barker P, Thackray K, et al. Mitochondrial dysfunction in patients with primary congenital insulin resistance. J Clin Invest 2011;121:2457–2461
27. Brehm A, Krssák M, Schmid AI, Nowotny P, Waldhäusl W, Roden M. Acute elevation of plasma lipids does not affect ATP synthesis in human skeletal muscle. Am J Physiol Endocrinol Metab 2010;299:E33–E38
28. Brehm A, Krssak M, Schmid AI, Nowotny P, Waldhäusl W, Roden M. Increased lipid availability impairs insulin-stimulated ATP synthesis in human skeletal muscle. Diabetes 2006;55:136–140
29. Szendroedi J, Schmid AI, Chmelik M, et al. Muscle mitochondrial ATP synthesis and glucose transport/phosphorylation in type 2 diabetes. PLoS Med 2007;4:e154
30. Lim EL, Hollingsworth KG, Smith FE, Thelwall PE, Taylor R. Effects of raising muscle glycogen synthesis rate on skeletal muscle ATP turnover rate in type 2 diabetes. Am J Physiol Endocrinol Metab 2011;301:E1155–E1162
31. Szendroedi J, Schmid AI, Meyerspeer M, et al. Impaired mitochondrial function and insulin resistance of skeletal muscle in mitochondrial diabetes. Diabetes Care 2009;32:677–679
32. Szendroedi J, Zwettler E, Schmid AI, et al. Reduced basal ATP synthetic flux of skeletal muscle in patients with previous acromegaly. PLoS ONE 2008;3:e3958
33. Schmid AI, Szendroedi J, Chmelik M, Krssák M, Moser E, Roden M. Liver ATP synthesis is lower and relates to insulin sensitivity in patients with type 2 diabetes. Diabetes Care 2011;34:448–453
34. Schmid AI, Chmelík M, Szendroedi J, et al. Quantitative ATP synthesis in human liver measured by localized ^{31}P spectroscopy using the magnetization transfer experiment. NMR Biomed 2008;21:437–443
35. Lei H, Ugurbil K, Chen W. Measurement of unidirectional Pi to ATP flux in human visual cortex at 7 T by using in vivo ^{31}P magnetic resonance spectroscopy. Proc Natl Acad Sci USA 2003;100:14409–14414
36. Du F, Zhu XH, Qiao H, Zhang X, Chen W. Efficient in vivo ^{31}P magnetization transfer approach for noninvasively determining multiple kinetic parameters and metabolic fluxes of ATP metabolism in the human brain. Magn Reson Med 2007;57:103–114
37. Du F, Zhu XH, Zhang Y, et al. Tightly coupled brain activity and cerebral ATP metabolic rate. Proc Natl Acad Sci USA 2008;105:6409–6414
38. Campbell-Burk SL, Jones KA, Shulman RG. ^{31}P NMR saturation-transfer measurements in Saccharomyces cerevisiae: characterization of phosphate exchange reactions by iodoacetate and antimycin A inhibition. Biochemistry 1987;26:7483–7492
39. Kingsley-Hickman PB, Sako EY, Mohanakrishnan P, et al. ^{31}P NMR studies of ATP synthesis and hydrolysis kinetics in the intact myocardium. Biochemistry 1987;26:7501–7510
40. Brindle KM, Radda GK. ^{31}P-NMR saturation transfer measurements of exchange between Pi and ATP in the reactions catalysed by glyceraldehyde-3-phosphate dehydrogenase and phosphoglycerate kinase in vitro. Biochim Biophys Acta 1987;928:45–55
41. LaNoue KF, Jeffries FM, Radda GK. Kinetic control of mitochondrial ATP synthesis. Biochemistry 1986;25:7667–7675
42. Mitsumori F, Rees D, Brindle KM, Radda GK, Campbell ID. ^{31}P-NMR saturation transfer studies of aerobic Escherichia coli cells. Biochim Biophys Acta 1988;969:185–193
43. Sheldon JG, Williams SP, Fulton AM, Brindle KM. ^{31}P NMR magnetization transfer study of the control of ATP turnover in Saccharomyces cerevisiae. Proc Natl Acad Sci USA 1996;93:6399–6404
44. Kemp GJ. The interpretation of abnormal ^{31}P magnetic resonance saturation transfer measurements of Pi/ATP exchange in insulin-resistant skeletal muscle. Am J Physiol Endocrinol Metab 2008;294:643–644
45. From AH, Ugurbil K. Standard magnetic resonance-based measurements of the Pi→ATP rate do not index the rate of oxidative phosphorylation in cardiac and skeletal muscles. Am J Physiol Cell Physiol 2011;301:C1–C11
46. Balaban RS, Koretsky AP. Interpretation of ^{31}P NMR saturation transfer experiments: what you can't see might confuse you. Focus on "Standard magnetic resonance-based measurements of the Pi→ATP rate do not index the rate of oxidative phosphorylation in cardiac and skeletal muscles". Am J Physiol Cell Physiol 2011;301:C12–C15
47. Brindle KM. ^{31}P NMR magnetization-transfer measurements of flux between inorganic phosphate and adenosine 5′-triphosphate in yeast cells genetically modified to overproduce phosphoglycerate kinase. Biochemistry 1988;27:6187–6196
48. van den Broek NM, Ciapaite J, De Feyter HM, et al. Increased mitochondrial content rescues in vivo muscle oxidative capacity in long-term high-fat-diet-fed rats. FASEB J 2010;24:1354–1364
49. Laurent D, Yerby B, Deacon R, Gao J. Diet-induced modulation of mitochondrial activity in rat muscle. Am J Physiol Endocrinol Metab 2007;293:E1169–E1177
50. Vidal-Puig AJ, Grujic D, Zhang CY, et al. Energy metabolism in uncoupling protein 3 gene knockout mice. J Biol Chem 2000;275:16258–16266
51. Wang S, Subramaniam A, Cawthorne MA, Clapham JC. Increased fatty acid oxidation in transgenic mice overexpressing UCP3 in skeletal muscle. Diabetes Obes Metab 2003;5:295–301
52. Cadenas S, Echtay KS, Harper JA, et al. The basal proton conductance of skeletal muscle mitochondria from transgenic mice overexpressing or lacking uncoupling protein-3. J Biol Chem 2002;277:2773–2778
53. Choi CS, Fillmore JJ, Kim JK, et al. Overexpression of uncoupling protein 3 in skeletal muscle protects against fat-induced insulin resistance. J Clin Invest 2007;117:1995–2003

54. Befroy DE, Falk Petersen K, Rothman DL, Shulman GI. Assessment of in vivo mitochondrial metabolism by magnetic resonance spectroscopy. Methods Enzymol 2009;457:373–393
55. Morino K, Petersen KF, Dufour S, et al. Reduced mitochondrial density and increased IRS-1 serine phosphorylation in muscle of insulin-resistant offspring of type 2 diabetic parents. J Clin Invest 2005;115:3587–3593
56. Befroy DE, Petersen KF, Shulman GI, Rothman DL. Localized 31P saturation transfer reveals differences in gastrocnemius and soleus rates of ATP synthesis in-vivo. Proc Int Soc Magn Reson Med 2008;2565
57. Pette D, Spamer C. Metabolic properties of muscle fibers. Fed Proc 1986; 45:2910–2914
58. Hoppeler H, Hudlicka O, Uhlmann E. Relationship between mitochondria and oxygen consumption in isolated cat muscles. J Physiol 1987;385:661–675
59. He J, Watkins S, Kelley DE. Skeletal muscle lipid content and oxidative enzyme activity in relation to muscle fiber type in type 2 diabetes and obesity. Diabetes 2001;50:817–823
60. Essén B, Jansson E, Henriksson J, Taylor AW, Saltin B. Metabolic characteristics of fibre types in human skeletal muscle. Acta Physiol Scand 1975;95:153–165
61. Bergh U, Thorstensson A, Sjödin B, Hulten B, Piehl K, Karlsson J. Maximal oxygen uptake and muscle fiber types in trained and untrained humans. Med Sci Sports 1978;10:151–154
62. Capó LA, Sillau AH. The effect of hyperthyroidism on capillarity and oxidative capacity in rat soleus and gastrocnemius muscles. J Physiol 1983;342:1–14
63. Short KR, Nygren J, Barazzoni R, Levine J, Nair KS. T(3) increases mitochondrial ATP production in oxidative muscle despite increased expression of UCP2 and -3. Am J Physiol Endocrinol Metab 2001;280:E761–E769
64. Winder WW, Baldwin KM, Terjung RL, Holloszy JO. Effects of thyroid hormone administration on skeletal muscle mitochondria. Am J Physiol 1975;228:1341–1345
65. Levine S. Role of tissue hypermetabolism in stimulation of ventilation by dinitrophenol. J Appl Physiol 1977;43:72–74
66. Saiki C, Mortola JP. Effect of 2,4-dinitrophenol on the hypometabolic response to hypoxia of conscious adult rats. J Appl Physiol 1997;83:537–542
67. Hood DA, Gorski J, Terjung RL. Oxygen cost of twitch and tetanic isometric contractions of rat skeletal muscle. Am J Physiol 1986;250:E449–E456
68. Chaumeil MM, Valette J, Guillermier M, et al. Multimodal neuroimaging provides a highly consistent picture of energy metabolism, validating ^{31}P MRS for measuring brain ATP synthesis. Proc Natl Acad Sci USA 2009; 106:3988–3993
69. Rooyackers OE, Adey DB, Ades PA, Nair KS. Effect of age on in vivo rates of mitochondrial protein synthesis in human skeletal muscle. Proc Natl Acad Sci USA 1996;93:15364–15369
70. Short KR, Vittone JL, Bigelow ML, Proctor DN, Nair KS. Age and aerobic exercise training effects on whole body and muscle protein metabolism. Am J Physiol Endocrinol Metab 2004;286:E92–E101
71. Navarro A, López-Cepero JM, Sánchez del Pino MJ. Skeletal muscle and aging. Front Biosci 2001;6:D26–D44
72. Ryan M, Ohlendieck K. Excitation-Contraction Uncoupling and Sarcopenia. Basic Appl Myol 2004;14:141–154
73. Pereira S, Marliss EB, Morais JA, Chevalier S, Gougeon R. Insulin resistance of protein metabolism in type 2 diabetes. Diabetes 2008;57:56–63
74. Halvatsiotis P, Short KR, Bigelow M, Nair KS. Synthesis rate of muscle proteins, muscle functions, and amino acid kinetics in type 2 diabetes. Diabetes 2002;51:2395–2404
75. Djurhuus MS, Vaag A, Klitgaard NA. Muscle sodium, potassium, and [(3) H]ouabain binding in identical twins, discordant for type 2 diabetes. J Clin Endocrinol Metab 2001;86:859–866
76. Landin K, Lindgärde F, Saltin B, Smith U. The skeletal muscle Na:K ratio is not increased in hypertension: evidence for the importance of obesity and glucose intolerance. J Hypertens 1991;9:65–69
77. Galuska D, Kotova O, Barrès R, Chibalina D, Benziane B, Chibalin AV. Altered expression and insulin-induced trafficking of Na+-K+-ATPase in rat skeletal muscle: effects of high-fat diet and exercise. Am J Physiol Endocrinol Metab 2009;297:E38–E49
78. Clausen T, Van Hardeveld C, Everts ME. Significance of cation transport in control of energy metabolism and thermogenesis. Physiol Rev 1991;71: 733–774
79. From AH, Zimmer SD, Michurski SP, et al. Regulation of the oxidative phosphorylation rate in the intact cell. Biochemistry 1990;29:3731–3743
80. Wilson DF. Factors affecting the rate and energetics of mitochondrial oxidative phosphorylation. Med Sci Sports Exerc 1994;26:37–43
81. Prompers JJ, Jeneson JA, Drost MR, Oomens CC, Strijkers GJ, Nicolay K. Dynamic MRS and MRI of skeletal muscle function and biomechanics. NMR Biomed 2006;19:927–953
82. Paganini AT, Foley JM, Meyer RA. Linear dependence of muscle phosphocreatine kinetics on oxidative capacity. Am J Physiol 1997;272:C501–C510
83. McCully KK, Fielding RA, Evans WJ, Leigh JS Jr, Posner JD. Relationships between in vivo and in vitro measurements of metabolism in young and old human calf muscles. J Appl Physiol 1993;75:813–819
84. Larson-Meyer DE, Newcomer BR, Hunter GR, Joanisse DR, Weinsier RL, Bamman MM. Relation between in vivo and in vitro measurements of skeletal muscle oxidative metabolism. Muscle Nerve 2001;24:1665–1676
85. Lanza IR, Bhagra S, Nair KS, Port JD. Measurement of human skeletal muscle oxidative capacity by ^{31}P-MR spectroscopy: a cross-validation with in vitro measurements. J Magn Reson Imaging 2011;34:1143–1150
86. Scheuermann-Freestone M, Madsen PL, Manners D, et al. Abnormal cardiac and skeletal muscle energy metabolism in patients with type 2 diabetes. Circulation 2003;107:3040–3046
87. Schrauwen-Hinderling VB, Kooi ME, Hesselink MK, et al. Impaired in vivo mitochondrial function but similar intramyocellular lipid content in patients with type 2 diabetes mellitus and BMI-matched control subjects. Diabetologia 2007;50:113–120
88. De Feyter HM, van den Broek NM, Praet SF, Nicolay K, van Loon LJ, Prompers JJ. Early or advanced stage type 2 diabetes is not accompanied by in vivo skeletal muscle mitochondrial dysfunction. Eur J Endocrinol 2008;158:643–653
89. De Feyter HM, Lenaers E, Houten SM, et al. Increased intramyocellular lipid content but normal skeletal muscle mitochondrial oxidative capacity throughout the pathogenesis of type 2 diabetes. FASEB J 2008;22: 3947–3955
90. van den Broek NM, Ciapaite J, Nicolay K, Prompers JJ. Comparison of in vivo postexercise phosphocreatine recovery and resting ATP synthesis flux for the assessment of skeletal muscle mitochondrial function. Am J Physiol Cell Physiol 2010;299:C1136–C1143
91. Quistorff B, Johansen L, Sahlin K. Absence of phosphocreatine resynthesis in human calf muscle during ischaemic recovery. Biochem J 1993; 291:681–686
92. Forbes SC, Paganini AT, Slade JM, Towse TF, Meyer RA. Phosphocreatine recovery kinetics following low- and high-intensity exercise in human triceps surae and rat posterior hindlimb muscles. Am J Physiol Regul Integr Comp Physiol 2009;296:R161–R170
93. Crowther GJ, Kemper WF, Carey MF, Conley KE. Control of glycolysis in contracting skeletal muscle. II. Turning it off. Am J Physiol Endocrinol Metab 2002;282:E74–E79
94. Walsh B, Tonkonogi M, Söderlund K, Hultman E, Saks V, Sahlin K. The role of phosphorylcreatine and creatine in the regulation of mitochondrial respiration in human skeletal muscle. J Physiol 2001;537:971–978
95. Harkema SJ, Meyer RA. Effect of acidosis on control of respiration in skeletal muscle. Am J Physiol 1997;272:C491–C500
96. Roussel M, Bendahan D, Mattei JP, Le Fur Y, Cozzone PJ. 31P magnetic resonance spectroscopy study of phosphocreatine recovery kinetics in skeletal muscle: the issue of intersubject variability. Biochim Biophys Acta 2000;1457:18–26
97. Walter G, Vandenborne K, Elliott M, Leigh JS. In vivo ATP synthesis rates in single human muscles during high intensity exercise. J Physiol 1999; 519:901–910
98. Iotti S, Frassineti C, Sabatini A, Vacca A, Barbiroli B. Quantitative mathematical expressions for accurate in vivo assessment of cytosolic [ADP] and DeltaG of ATP hydrolysis in the human brain and skeletal muscle. Biochim Biophys Acta 2005;1708:164–177
99. Arnold DL, Matthews PM, Radda GK. Metabolic recovery after exercise and the assessment of mitochondrial function in vivo in human skeletal muscle by means of ^{31}P NMR. Magn Reson Med 1984;1:307–315
100. van den Broek NM, De Feyter HM, de Graaf L, Nicolay K, Prompers JJ. Intersubject differences in the effect of acidosis on phosphocreatine recovery kinetics in muscle after exercise are due to differences in proton efflux rates. Am J Physiol Cell Physiol 2007;293:C228–C237
101. Schmid AI, Schrauwen-Hinderling VB, Andreas M, Wolzt M, Moser E, Roden M. Comparison of measuring energy metabolism by different (31) P-magnetic resonance spectroscopy techniques in resting, ischemic, and exercising muscle. Magn Reson Med 2012;67:898–905
102. Sugden PH, Smith DM. The effects of glucose, acetate, lactate and insulin on protein degradation in the perfused rat heart. Biochem J 1982; 206:467–472
103. Overmoyer BA, McLaren CE, Brittenham GM. Uniformity of liver density and nonheme (storage) iron distribution. Arch Pathol Lab Med 1987;111: 549–554
104. Taylor DJ, Styles P, Matthews PM, et al. Energetics of human muscle: exercise-induced ATP depletion. Magn Reson Med 1986;3:44–54